Development of an OpenFOAM model for the Molten Salt Fast Reactor transient analysis

Manuele Aufiero [a], Antonio Cammi [a], Olivier Geoffroy [b], Mario Losa [a], Lelio Luzzi [a,*], Marco E. Ricotti [a], Hervé Rouch [b]

[a] *Politecnico di Milano - Department of Energy - CeSNEF (Enrico Fermi Center for Nuclear Studies), via Ponzio, 34/3, 20133 Milano, Italy*
[b] *INOPRO – Tlspace Vercors, 118, chemin des Breux, 38250 Villard de Lans, France*

Received 19 November 2013
Received in revised form
21 February 2014
Accepted 4 March 2014
Available online 12 March 2014

1. Introduction

Traditionally, nuclear reactor analysis is performed by coupling neutron kinetics and thermal-hydraulic codes (Avramova and Ivanov, 1997). These coupled codes techniques are often based on the "operator-splitting" approach in which the time-dependent solution is reached using the output from one code (e.g., the neutron kinetics code) as input to another code (e.g., the thermal-hydraulic code) at each time step. Often, the nonlinearities due to the coupling are not resolved in the time step, possibly reducing the overall accuracy (Ragusa and Mahadevan, 2009; Mahadevan et al., 2012).

In MSRs, the presence of strong coupling between the different phenomena calls for the adoption of suitable modelling approaches, while performing reactor analysis (see, e.g., Special Section: MSR and FHR of *Annals of Nuclear Energy*, vol. 64, 2014). A detailed description and comparison of recent works related to MSR multi-physics modelling is given in a previous paper of some of the authors (Cammi et al., 2011). More recently, at Politecnico di Milano, a coupled model for the Molten Salt Fast Reactor (MSFR) has been developed adopting the mutiphysics code COMSOL. That model has been recently compared to an in-house code developed at Delft

* Corresponding author.
E-mail address: lelio.luzzi@polimi.it (L. Luzzi).

University of Technology showing a good agreement for several transient case studies (Fiorina et al., 2014).

Both models (COMSOL and TUDelft) rely on multi-group diffusion for the neutronics and involve a simplified, two-dimensional (2D) axial-symmetric representation of the MSFR. This approximation is considered to be appropriate for the purpose of preliminary transient analyses. Nonetheless, there are several situations in which a full-core three-dimensional (3D) representation of the primary circuit is desirable. Namely asymmetric transients (e.g., single pump failure) cannot be properly simulated with 2D simulations. Moreover, recent studies of some of the authors (INOPRO, e.g., see Brovchenko et al., 2013) highlighted the fact that in some of the expected operating conditions of the MSFR, the 2D axial-symmetric approximation of the turbulent flow might lead to a prediction of the flow structures with significant differences with respect to results obtained from accurate 3D simulations of the rector core. These differences in the turbulent viscosity and velocity fields have major impact on the fuel temperature distribution in the core, which is a key parameter for the reactor analysis in both nominal and accidental conditions.

In this paper, the development and assessment of a multiphysics model devoted to the transient analysis of the Molten Salt Fast Reactor is discussed[1] More in general, the proposed tool is aimed at studying the dynamic behaviour of non-moderated MSRs. Its distinguishing feature, with respect to previous works available in the literature (e.g., see Fiorina et al., 2014), is the capability to deal with full-core 3D analysis, while allowing an accurate description of the in-core turbulent fuel flow and limiting the demand for computational resources. For this purpose, a specific modelling approach has been developed, adopting the multiphysics toolkit OpenFOAM (Weller et al., 1998). The work is focused on the implementation of accurate and consistent time-integration and coupling techniques, and the adoption of strategies for the reduction of computational requirements. The main purpose of the proposed model is to serve as fast-running computational tool in the phase of design optimization of fuel loop components. More in general, the present tool is of valuable help to investigate the peculiarities of the reactor physics of circulating-fuel systems, especially in the presence of thermal feedbacks on neutronics. Detailed safety analysis is beyond the scope of the present work and would require layout specifications of the core and fuel circuit components, which are not available in this pre-conceptual design of the MSFR.

Recently, the multi-group neutron diffusion approximation has been successfully adopted in OpenFOAM for both forward and adjoint calculations in the MSFR (Aufiero et al., 2014), thanks to the work on block-coupled solver implementation of Clifford and Jasak (2009). Nonetheless, in the present work, in order to reduce the computational requirements, the one-speed diffusion approximation has been preferred, along with the adoption of suitable albedo boundary conditions, which limit the computational domain to the fuel circuit only. The suitability of this simplifications has been verified through a comparison of the shape of the scalar flux between the OpenFOAM model and Monte Carlo simulations, whereas the time-dependent response of the model to a super-prompt-critical reactivity insertion has been compared to results from the aforementioned COMSOL and TUDelft models.

The paper is organized as follows. In Section 2, the investigated reactor concept is briefly presented. In Section 3, the adopted methodology is discussed. In Section 4, the assessment of the developed model against other tools is presented, along with results from a pump failure simulation. Conclusions are drawn in Section 5.

[1] The multiphysics solver has been preliminary presented at the 7th OpenFOAM Workshop (Darmstadt, June, 2012) — for further details see Aufiero (2014). http://www.openfoamworkshop.org/2012/downloads/Workshop-Documents/Presentations-Talks/AufieroManuele/final_ManueleAufieroSlidesOFW7.pdf.

2. Investigated reactor concept

2.1. The Molten Salt Fast Reactor

The Molten Salt Fast Reactor (MSFR) is the reference circulating-fuel reactor in the framework of the Generation IV International Forum (GIF, 2010; Serp et al., in press), and it is mainly developed in the EURATOM EVOL (Evaluation and Viability Of Liquid fuel fast reactor system) Project (EVOL, 2010–2013). Details about the MSFR configuration can be found in the references (Merle-Lucotte et al., 2009, 2011; Brovchenko et al., 2012). In the following, a brief description of the reactor is given. Fig. 1 shows a schematic view of the MSFR components, the fuel salt being not pictured. The molten salt mixture of the fuel circuit acts both as fuel and coolant. The core of the reactor has a volume of 9 m^3. The fuel salt enters from the bottom and is extracted from the top of the core. The heated mixture flows in 16 external loops where it exchanges heat with an intermediate salt and is pumped back to the core. The fraction of the fuel salt in the core is approximately 50%, and the average nominal in-core temperature is 700 °C. Above and below the core, nickel-based alloy reflectors are present in order to improve neutron economy. Radially, the core is surrounded by a fertile salt containing a thorium and a lithium fluoride salt in order to improve the breeding performance of the reactor. In Table 1, the main design parameters of the MSFR are listed.

2.2. Geometry

The preliminary choice of a square-cylindrical shape for the MSFR comes primarily from the neutron economy point of view (Merle-Lucotte et al., 2009, 2011). In nominal flow-rate conditions, large recirculation vortices appear near the core wall when this

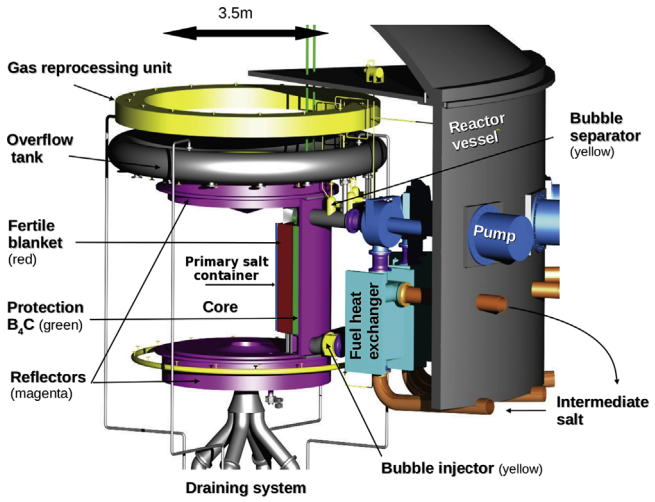

Fig. 1. Schematic representation of the MSFR fuel loop (Brovchenko et al., 2012).

Table 1
Nominal design parameters of the MSFR.

Thermal power	3000 MW
Core inlet temperature	650 °C
Core outlet temperature	750 °C
Fuel salt composition	
LiF– ThF_4–$^{233}UF_4$	77.5–20–2.5 mol%
Fuel salt volume	18 m^3
In-core fuel fraction	50%
Fuel salt circulation period	4 s

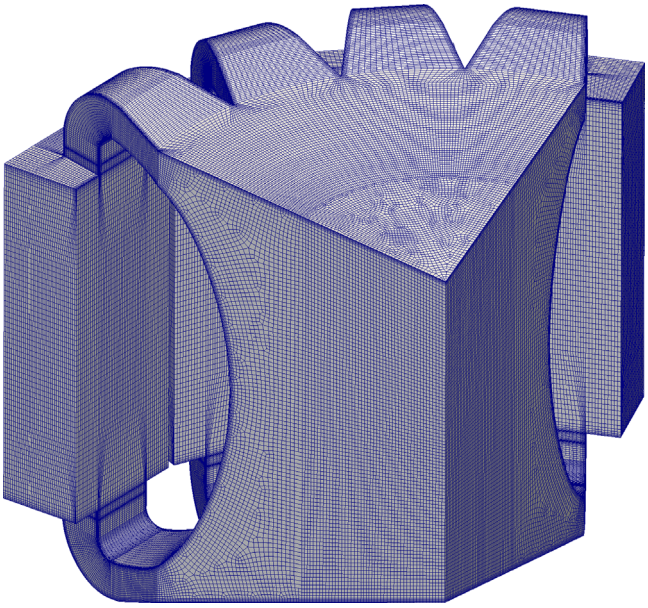

Fig. 2. Spatial mesh adopted for the modelling of the MSFR fuel circuit.

shape is considered, which might lead to excessive structural material temperatures. For this reason, a core shape optimization process is ongoing within the EVOL Project (Rouch et al., 2014), aimed at the elimination of high-temperature zones. This issue and the strong influence of the CFD modelling on the prediction of the MSFR behaviour (Losa, 2013) call for the adoption of realistic three-dimensional geometries, while performing multiphysics transient or steady-state reactor analysis. In this work, the "toroidal-shaped" geometry proposed in the EVOL Project has been adopted (Brovchenko et al., 2013; Rouch et al., 2014). In Fig. 2, a spatial finite-volume mesh adopted for the modelling of one-quarter of the MSFR is shown. The "toroidal" reshaping of the radial fuel salt container to avoid recirculation is clearly visible along with four external loops. In Section 4, the simulation of a single pump failure scenario is presented. In order to catch the effect of asymmetrical in-core flow pattern, the results have been obtained adopting a full-core 3D geometry.

3. Modelling approach

In this section, the methodologies adopted in the development of the proposed model are described and discussed.

3.1. The multiphysics toolkit OpenFOAM

In this work, the multiphysics open-source toolkit OpenFOAM (Weller et al., 1998; Jasak et al., 2007) is adopted to spatially discretize and numerically solve the equations related to neutron diffusion, delayed neutron precursor transport, energy balance and fluid flow using standard finite-volume methods (the main equations implemented in the model are reported in the Appendix). The OpenFOAM C++ library is featured by automatic matrix construction and solution capabilities for scalar and vector equations, adopting several possible differencing and interpolation schemes. For this reason, its adoption is particularly suitable for the modelling of complex coupled phenomena. In addition to the ease of implementing the constitutive equations of different physical phenomena, OpenFOAM is provided by different pre-implemented models and solvers for the simulation of fluid flows. This allowed us to focus the development efforts on the implementation and verification of the neutronics and delayed neutron precursors models and on the multiphysics coupling and time integration strategies. The presented model has been developed starting from the standard *buoyantBoussinesqPimpleFoam* solver available in OpenFOAM 2.2.1.

3.2. Fluid-dynamics and heat transfer modelling

The model of the fluid flow (molten salt mixture) is based on the Reynolds-Averaged Navier–Stokes (RANS) equations for mass and momentum conservations. In the present work, the standard and the *realizable k*-epsilon turbulence models for incompressible flows have been adopted along with the standard wall function treatment. Detailed CFD analyses of both the 2D and 3D core geometry have been performed in previous works (Losa, 2013; Rouch et al., 2014), and are beyond the scope of the present work. The buoyancy effects have been taken into account through the Boussinesq approximation.

The classical energy balance equation (Eq. (7) in Appendix) is solved for the calculation of the in-core temperature distribution. Turbulent heat diffusivity is considered and modelled from the turbulent viscosity, adopting an effective uniform value of the turbulent Prandtl number equal to 0.85 in the whole domain. The thermophysical properties of the molten salt mixture are considered constant and are relative to a fluid temperature of 700 °C. The main thermophysical quantities adopted are summarized in Table 2.

In order to reduce the computational effort, the heat transfer in structural materials and in the blanket has been neglected, thus, thermal insulation has been applied to the boundaries of the fuel circuit.

At present, the design specifications of the MSFR fuel circuit components (e.g., primary pumps and heat exchangers) are not fully defined. Within the EVOL Project there is an ongoing research activity aimed at the definition of the most suitable options. In the present work, in order to allow for the simulation of a wide range of accidental scenarios, a simplified description of the pumps and the heat exchangers has been introduced in the multiphysics model. The pumps have been simulated through a momentum source in the 16 out-of-core circuits. In order to accurately take into account the possible blockage of one or more pumps, the momentum sources have a dependency on the flow rate in each branch. In case of pump blockage, this acts as an additional head loss in the circuit. Lacking any detailed information about the pump characteristic, it has been assumed that the pressure loss due to a broken pump is proportional to the power of 2 of the flow rate and reaches a value of 1.5 bar at nominal flow rate. This approach, although very simplified, allows us to capture the main dynamics of the system in case of malfunctioning of the fuel circuit components. Moreover, it is consistent with previous works (Fiorina et al., 2014) and therefore allows for accurate comparisons with other models.

Due to the limited operating pressure of both the fuel circuit and the intermediate salt circuit, plate-type heat exchangers (HEX) are envisaged as possible option due to their compactness and simplicity. Following this option, the heat exchanger specifications (e.g., plate thickness, channel dimensions, etc.) have been preliminarily

Table 2
Fuel salt thermophysical properties adopted in the present work (Brovchenko et al., 2013).

Density	4125 kg m^{-3}
Kinematic viscosity	2.46×10^{-6} m^2 s^{-1}
Thermal conductivity	1.01 W m^{-1} K^{-1}
Coefficient of thermal expansion	2.14×10^{-4} K^{-1}

optimized by INOPRO within the EVOL Project, and are reported in Table 3. The optimization process has followed the criteria of a compromise aimed at the minimization of both the primary salt volume in the exchanger and the head losses. It resulted in a total fuel salt volume in the 16 heat exchangers of 6.8 m^3. Similar to what has been performed for the pumps, the HEX modelling has been introduced as 16 distributed sources of momentum and heat sinks. The pressure losses in the heat exchangers have been estimated for several flow rates through suitable correlations, also accounting for the changes in the flow regime. In a similar way, the heat exchange coefficient has been calculated for different operating conditions of both the fuel and the intermediate circuit. For the sake of simplicity, the dependency of the head losses and the heat exchange on the flow conditions has been introduced in the multiphysics model as a polynomial interpolation of the calculated points between 5% and 100% of the nominal flow. In Fig. 3, the calculated curves for the head losses and the heat exchange coefficient are depicted.

Table 3
Main specifications of the corrugated plate-type heat exchanger adopted in the present work.

Arrangement	Countercurrent flow
Plate thickness	2 mm
Channel width (fuel salt)	3 mm
Channel height	50 cm
Corrugation pattern angle	30 °C

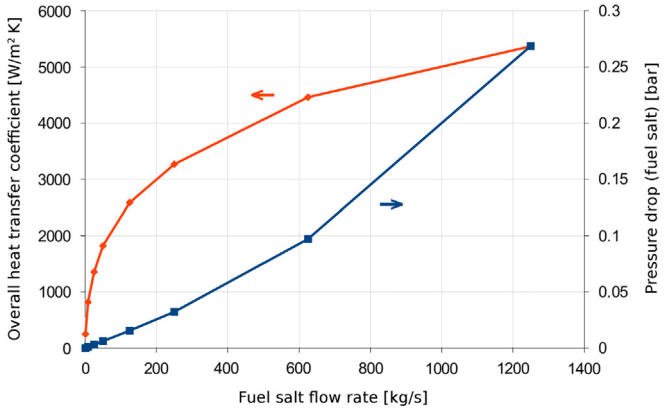

Fig. 3. Head loss and heat exchange coefficient in the heat exchanger as a function of the primary salt flow rate (intermediate salt at nominal flow rate).

3.3. Neutronics modelling

The one-speed neutron diffusion approximation (Duderstadt and Hamilton, 1976) is adopted for the modelling of the reactor neutronics (see Eq. (1) in Appendix). In order to further reduce the computational burden of the simulations, the albedo boundary conditions have been adopted both in the upper and lower limits of the core (axial reflectors) and in the radial wall (blanket salt). In this way, the solution of the neutron diffusion equation is limited to the fuel salt circuit, thus reducing the computational requirement of the calculations. The group constants adopted in the model have been calculated by means of the Monte Carlo code SERPENT (2011), adopting the JEFF-3.1 evaluated nuclear data library (Koning et al., 2006) and the fuel composition relative to the ^{233}U-started MSFR option (Merle-Lucotte et al., 2011). In order to take into account the thermal feedback on neutronics, a dependency of the cross sections on the fuel temperature and density has been introduced in the model. In particular, the Doppler effect is described through a logarithmic dependence of the fuel capture and fission cross sections, which has been calculated interpolating several Monte Carlo runs at different fuel temperatures. As mentioned in Section 3.2, the fluid flow in the fuel circuit is described adopting the incompressible Navier–Stokes equations. Nonetheless, in order to fully capture the effect of fuel thermal expansion on neutronics, a temperature-dependent effective fuel density is considered when solving the neutron diffusion equation. In particular, a linear dependency on the salt density has been introduced for the cross sections and the diffusion coefficient (Eqs. (2) and (3) in Appendix).

This simple and computationally lightweight neutronics model showed was able to accurately describe the space and time dependence of the neutron fluxes in the MSFR. In Fig. 4, the neutron flux is shown as a function of the axial and radial coordinates, as predicted by the OpenFOAM model and by the Monte Carlo code SERPENT. Note that the SERPENT estimates extend also in the blanket salt and in the axial reflectors, whereas the OpenFOAM calculations are limited to the fuel salt in the core. The two curves are in a good agreement (with maximum relative errors smaller than 3%) and the small discrepancies can be considered acceptable for the purpose of the present work.

The drift of delayed neutron precursors plays an important role in reactor dynamics of molten salt reactors. In the present model,

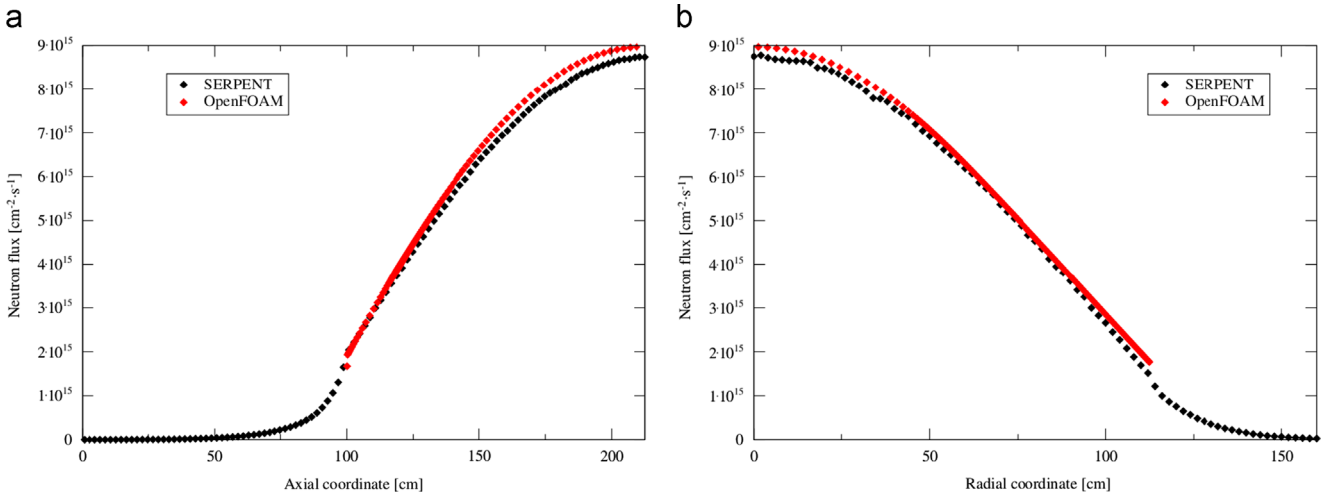

Fig. 4. Neutron flux as a function of the axial (a) and radial (b) coordinates, as predicted by the OpenFOAM model and by the Monte Carlo code SERPENT.

the balance equations for eight groups of precursors are adopted (see Eq. (5) in Appendix). The decay constants of the delayed neutron precursors are taken from the JEFF-3.1 library (Koning et al., 2006). Due to the adoption of the one-group approximation, the effective (adjoint weighted) delayed neutron fractions ($\beta_{eff,i}$) were considered instead of the physical delayed neutron fractions ($\beta_{0,i}$). This allowed us to take into account the different effectiveness of delayed and prompt neutrons, due to emission spectra, under the assumption that energy and spatial effects can be separated. This simplifying approximation has proved accurate in the case of the MSFR (Aufiero et al., 2014). The $\beta_{eff,i}$ values have been calculated by means of SERPENT and are shown in Table 4 along with the respective decay constants (λ_i) adopted in the present work.

Also, the modelling of the decay heat is introduced by means of the superposition of three exponentially decaying terms. These terms are obtained by a curve fitting on the output of a SERPENT burn-up simulation, also allowing for on-line fuel reprocessing and bubbling extraction of gaseous fission products (Aufiero et al., 2013). In Fig. 5, the decay heat curve for the ^{233}U-started MSFR after long operation at nominal power is shown for the first 5 min. The decay heat is expressed as fraction of the nominal power. The black dots represent SERPENT results. The red line represents the exponential interpolation adopted in this work. The blue dots show the modulus of the relative interpolation error. The choice of three terms represents a compromise between the accuracy in the description of the decay heat curve and computational requirements. This approximation can be judged appropriately for transient simulations that are limited to a time scale of several minutes. Both decay heat and delayed neutron precursors are transported by the fluid flow. It has been recently pointed out (Aufiero et al., 2014) that the turbulent diffusion of delayed neutron precursors might have a non-negligible effect on the effective delayed neutron fraction and thus on reactor kinetics. For this reason, in addition to the convective term, turbulent diffusion is also considered for these quantities, adopting a turbulent Schmidt number of 0.85.

Table 4
Effective delayed neutron fractions and decay constants.

Group	$\beta_{eff,i}$ (pcm)	λ_i (s^{-1})
1	21.8	1.25×10^2
2	47.6	2.83×10^2
3	39.3	4.25×10^2
4	63.5	1.33×10^1
5	103.5	2.92×10^1
6	18.1	6.66×10^1
7	22.8	1.63
8	5.2	3.55

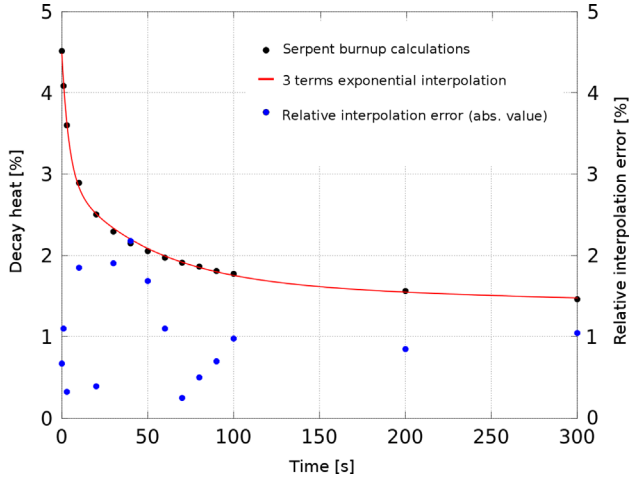

Fig. 5. Decay heat as a function of time. ^{233}U-started MSFR after long operation. SERPENT burnup calculations and 3 terms exponential interpolation. (For interpretation of the references to colour in this figure caption, the reader is referred to the web version of this paper.)

The effect of the fuel motion on neutron kinetics and on the general reactor behaviour is intrinsically caught in the present model, which features the explicit solution of the precursors balance equations coupled to the salt velocity and turbulence fields. The influence of the fuel circulation period on kinetics parameters has been examined in detail in a previous work of the authors (Aufiero et al., 2014) along with a sensitivity study on the effect of the turbulent Schmidt number.

CFD and neutronics equations are solved adopting the same spatial mesh. This allowed the adoption of a simple and computationally efficient cell-wise spatial coupling of the different variables, without needing the implementation of mesh mapping techniques. In the next section, the scheme adopted for the time-coupling of the different variables is described.

3.4. Time integration scheme and multiphysics coupling technique

In general, the coupled neutronics/thermal-hydraulics problem involves the solution of particularly stiff equations and is featured by the presence of fast time scale modes, hence the choice of an implicit time integration scheme appears mandatory. This is particularly true in the case of the Molten Salt Fast Reactor in which the average prompt neutron lifetime is in the order of 1 μs (Fiorina et al., 2013). Moreover, the possibility of adopting accurate higher order integration techniques might be useful in many relevant situations. For these reasons, the adoption of implicit Runge–Kutta methods has been preferred in this work. In particular, a 6 stage, fourth order explicit, singly diagonally implicit Runge–Kutta (ESDIRK) scheme from Kennedy and Carpenter (2003) was adopted. This scheme (presented in Table 5) also features an embedded third order error estimator, which might be used for evaluating the time integration accuracy, also in view of adaptive time-stepping.

The conventional operator-splitting technique adopted in reactor analysis involves the sequential solution of the different physics, once per time step. While this technique might offer several practical advantages, it is “nonlinearly inconsistent” in the coupling (Ragusa and Mahadevan, 2009) and might lead to inaccurate results in case of strong feedback between the physics as in the case of the present work.

Among the various techniques available to fully solve the non-linearities due to the coupling of the different phenomena, the adoption of Picard iterations has been preferred for the simplicity of implementation and verification. At each implicit stage of the ESDIRK scheme, all the equations are iteratively solved and the coupling terms are updated at each sweep, until the residuals of any physics drop below a user-defined tolerance. After the solution of the last stage, both the third order and fourth order estimates of the solution for all the variables are available, whose comparison might be adopted as error estimate. While this method might be outperformed by more efficient techniques, it offers the possibility to adopt optimized linear solvers for each physics and allows for a simpler verification of both the single-physics and the whole code implementation. This was considered of primary importance also because of the little availability of both well assessed multiphysics solvers for MSRs and experimental data on fast system, similar to the MSFR.

In Fig. 6, the reactor power after a reactivity insertion of 150 pcm (about 1$) from nominal, steady state conditions is shown. Reactivity has been introduced by means of a direct, step-wise perturbation of the fission cross-section. This transient involves a rapid power rise

Table 5
Butcher table of the adopted explicit, singly diagonally implicit Runge–Kutta integrator with embedded error estimator (Kennedy and Carpenter, 2003).

c_i	a_{ij}					
0	0					
$\frac{1}{2}$	$\frac{1}{4}$	$\frac{1}{4}$				
$\frac{83}{250}$	$\frac{8611}{62\,500}$	$\frac{1743}{31\,250}$	$\frac{1}{4}$			
$\frac{31}{50}$	$\frac{5\,012\,029}{34\,652\,500}$	$\frac{654\,441}{2\,922\,500}$	$\frac{174\,375}{388\,108}$	$\frac{1}{4}$		
$\frac{17}{20}$	$\frac{15\,267\,082\,809}{155\,376\,265\,600}$	$\frac{71\,443\,401}{120\,774\,400}$	$\frac{730\,878\,875}{902\,184\,768}$	$\frac{2\,285\,395}{8\,070\,912}$	$\frac{1}{4}$	
1	$\frac{82\,889}{524\,892}$	0	$\frac{15\,625}{83\,664}$	$\frac{69\,875}{102\,672}$	$\frac{2260}{8211}$	$\frac{1}{4}$
b_i	$\frac{82\,889}{524\,892}$	0	$\frac{15\,625}{83\,664}$	$\frac{69\,875}{102\,672}$	$\frac{2260}{8211}$	$\frac{1}{4}$
b_i^*	$\frac{4\,586\,570\,599}{29\,645\,900\,160}$	0	$\frac{178\,811\,875}{945\,068\,544}$	$\frac{814\,220\,225}{1\,159\,782\,912}$	$\frac{3\,700\,637}{11\,593\,932}$	$\frac{61\,727}{225\,920}$

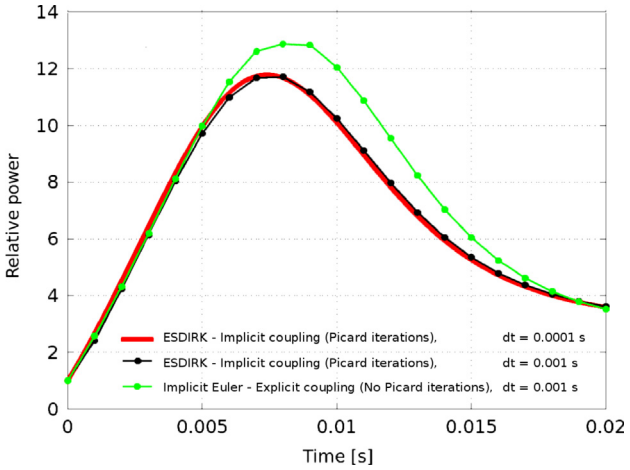

Fig. 6. 150 pcm reactivity insertion. Comparison between implicit and explicit coupling strategies. (For interpretation of the references to colour in this figure caption, the reader is referred to the web version of this paper.)

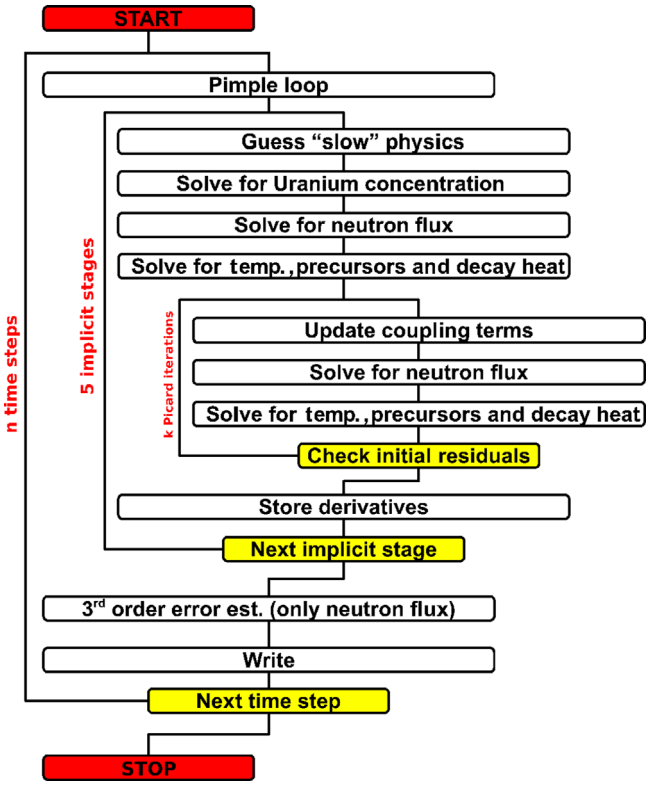

Fig. 7. Coupling scheme.

and a fast increase of temperature, which promptly induces negative neutronics feedbacks and reduces the power. The red line shows the results from a simulation with a constant time step of 1×10^{-4} s, adopting the time integration scheme described above (reference solution). The black dots were obtained adopting the same scheme and a time step of 1×10^{-3} s. It can be appreciated that both the power rise and the action of the negative reactivity feedbacks are accurately resolved. The green dots show results obtained with the operator-splitting approach, commonly adopted in nuclear reactor analysis: each physics is solved sequentially and the coupling terms are updated once per time step. Thanks to the implicit nature of the single-physics time integrators adopted, and despite the stiffness of the neutronics, even this coupling scheme is able to accurately describe the steep power increase. Nonetheless, when the dynamics of the system becomes dominated by the couplings between the physics (temperature feedbacks), the operator-splitting approach fails to accurately describe the transient evolution.

Different strategies have been tested in order to reduce the computation time of the coupled solver. The adoption of the classical Aitken acceleration technique gave limited improvements with a minor reduction of the total number of Picard iterations required to reach tolerances of practical interest for the purpose of the present analyses. On the other hand, the adoption of an accurate guess for the initial value of the unknown variables significantly improved the performance of the solver. In particular, the explicit Runge–Kutta scheme (ERK) associated with the adopted ESDIRK (Kennedy and Carpenter, 2003) has been employed at each implicit stage to estimate a first guess for the iterations sweep. This provided an efficient way to make use of the available information from the previous stages with a minimal computational cost.

The 3D modelling of the fluid flow in the MSFR proved to require fine spatial meshes in order to correctly catch the reactor behaviour

Table 6
Estimation of the multiplication factor (^{233}U-started MSFR option) for different fuel temperatures and densities. Comparison between SERPENT and OpenFOAM.

Configuration	SERPENT		OpenFOAM		Rel. diff. (O − S) / S
	k_{eff} (−)	Δk_{eff} (pcm)	k_{eff} (−)	Δk_{eff} (pcm)	Δk_{eff} (%)
Reference (T=900 K, ρ = 4.12 g cm^{-3})	0.99904 ± 0.00008	–	1.00619	–	–
ΔT = +300 K	0.98791 ± 0.00007	−1113 ± 11	0.99482	−1136	+2.1 ± 0.1
$\Delta\rho$ = −5%	0.99101 ± 0.00008	−803 ± 11	0.99843	−776	−3.3 ± 0.1

O, OpenFOAM results; S, SERPENT results.

(few millions of cells for the full-core model). In this condition, the solution for the variables related to the fluid flow (e.g., velocity, pressure, turbulent kinetic energy, etc.) requires a large amount of computational time. Considering also that in some of the transients of interest the time steps might be initially limited to few tens of μs, fully embedding the RANS equations in the integration scheme described above was considered too computationally expensive. For this reason, the solution for the fluid flow inside the reactor core has been obtained adopting the transient SIMPLE algorithm (Versteeg and Malalasekera, 2007), once per time step. The convective terms for the energy and precursors balance equations are kept constant during the time step. Several considerations were made in favour of the adoption of this simplification. In particular, it should be taken into account that in the fast transient, in which the coupling between the physics needs to be more accurately resolved (i.e., reactivity insertions close to or above prompt-criticality), the reactor response is dominated by the evolution of neutron fluxes, fuel temperature and delayed neutron precursors concentration. As a clarifying example, in the 200 pcm reactivity insertion presented as test case in Section 4, the reactor power reaches 150 times the nominal value, and is then reduced by a factor of ten by the strong reactivity feedbacks in about 0.01 s. In this time period, the fluid flow structures barely changed.

The general structure of the adopted coupling scheme is sketched in Fig. 7.

3.5. Initial steady-state conditions and parallel computing

In order to find the nominal steady-state conditions, the coupled neutronic-thermal hydraulic eigenvalue problem is solved iteratively adopting the standard power iteration method. In this way, it is possible to find the effective multiplication factor (k_{eff}) that brings the system to criticality by taking into account the spatial dependence in the core of both the fuel temperature field and the delayed neutron source distribution.

k_{eff} estimates provided by the OpenFOAM model have been compared to SERPENT results for simple reactor conditions in the 2D, axial-symmetric geometry, and are reported in Table 6. The capability to catch the main reactivity feedbacks is assessed via eigenvalue calculations at different fuel temperatures and densities. In the reference configuration, the fuel salt is considered with a uniform temperature of 900 K and density of 4.12 g cm^{-3}. In the second configuration considered, the fuel temperature has been increased to 1200 K to investigate Doppler effect. The third configuration involves a reduction of the fuel density of 5%. In Table 6, both the k_{eff} estimates in the three configurations, and the variations with respect to reference conditions are shown for the two tools. The OpenFOAM neutron diffusion model slightly overestimates the temperature reactivity feedback of about 2% with respect to SERPENT. On the other hand, the effect of increased leakages due to the fuel density change is underestimated of about 3.3%.

OpenFOAM offers the embedded capability to run applications in parallel thanks to the domain decomposition method. Fig. 8 shows an example of computational domain splitting: the fuel circuit is subdivided into different zones, and each one is assigned to a different processor core. The decomposition is performed automatically in pre-processing trying to minimize communication and imbalance between processors. In this way, the multiphysics solver can efficiently run in parallel. Although a systematic scalability study has not been preformed yet, the solver showed a good behaviour in all the parallel run tests.

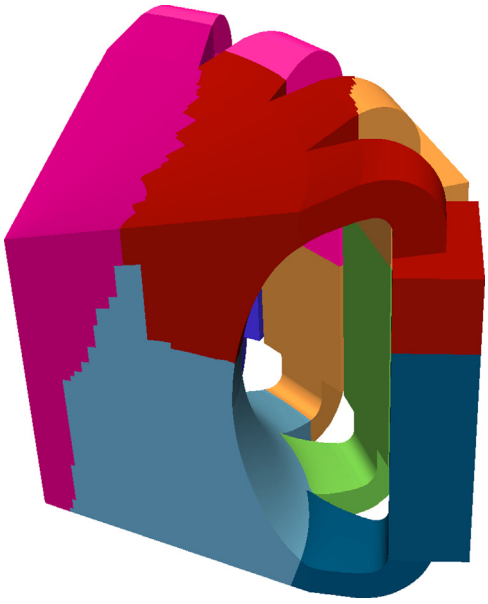

Fig. 8. Example of decomposed domain for parallel computing. Each zone is assigned to a different processor core.

In Section 4.1, results from a super prompt-critical reactivity insertion transient are shown. The 10 s simulation refers to a simple 2D geometry with about 2×10^5 cells. In order to give an idea of the typical running time for simple case studies, the simulation was run on a machine with an Intel® Xeon™ E5440 CPU with 8 cores and a clock speed of 2.83 GHz and was completed in approximately 1 h. For the sake of comparison, the COMSOL model with a similar number of degrees of freedom took approximately 22 h to run the transient on the same machine.[2]

4. Numerical results

4.1. Assessment against COMSOL and TUDelft models

The capability of the developed model has been assessed through a comparison with other multiphysics tools. Because no

[2] The COMSOL model features a different time integration technique (the third order backward differentiation formula), a different error estimation method and a different spatial discretization (finite element methods). For this reason, the computational performance of the two tools can be only roughly compared. The main limiting task for the COMSOL model has been found to be the solution of the turbulent flow (k-epsilon).

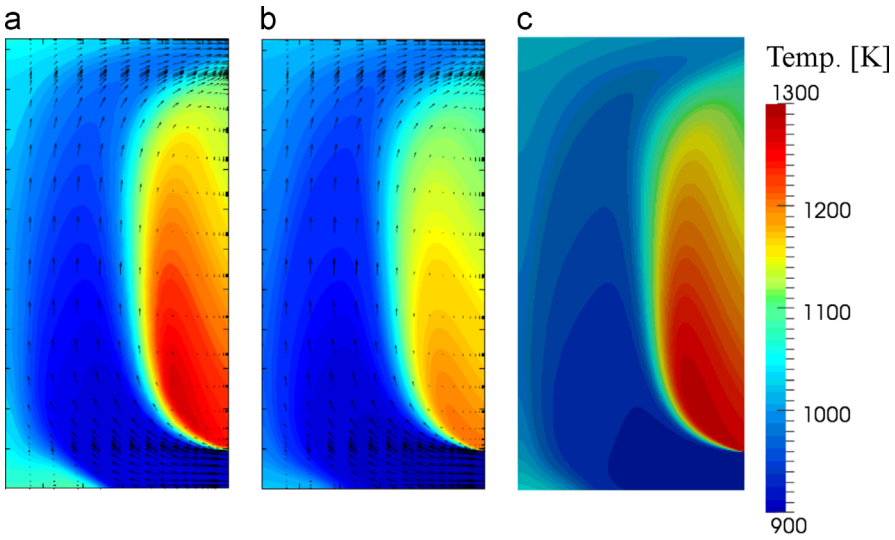

Fig. 9. Fuel temperature field at nominal conditions. Comparison among OpenFOAM, COMSOL and TUDelft models. Simplified 2D, axial-symmetric MSFR test case.

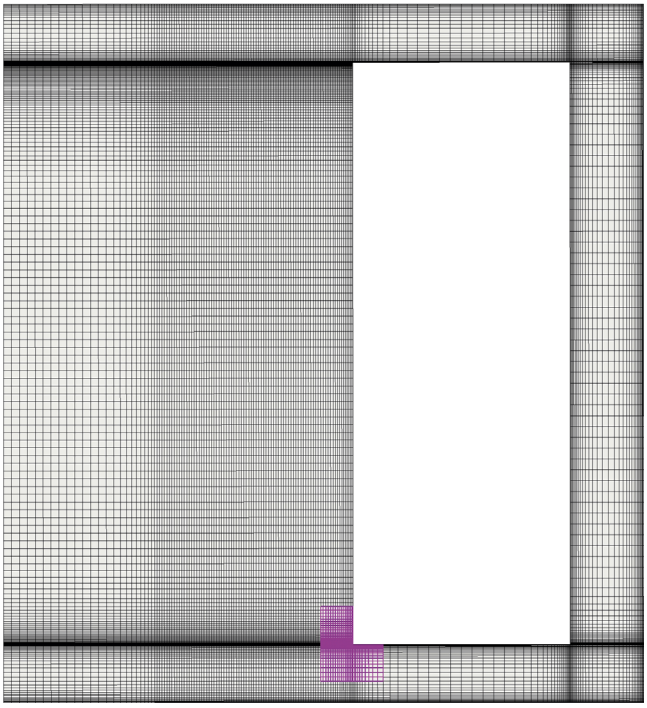

Fig. 10. 2D, axial-symmetric spatial mesh adopted in the OpenFOAM model.

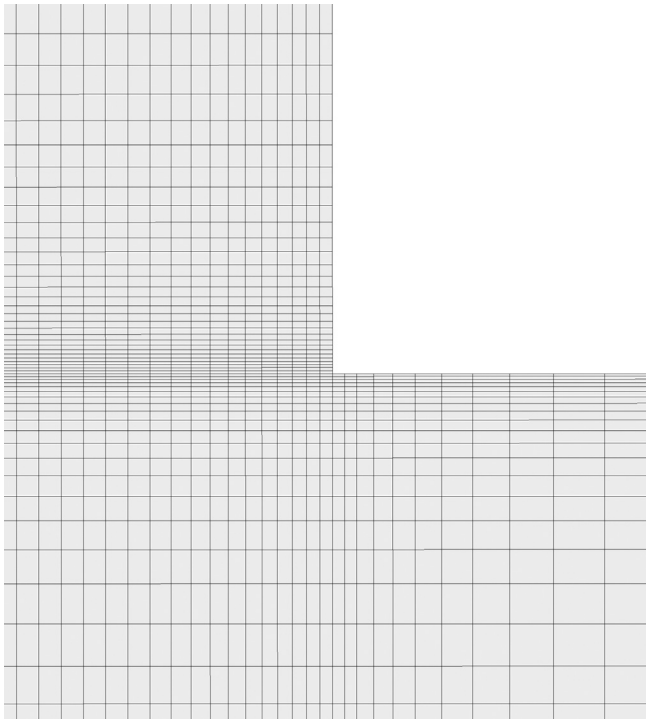

Fig. 11. 2D, axial-symmetric spatial mesh adopted in the OpenFOAM model (detail of the core inlet).

results are available in the open literature, which refers to 3D full-core simulations of non-moderated MSR on realistic geometries, the comparison has been carried out on a simplified case.

In Fig. 9, the nominal in-core temperature distribution, as predicted by OpenFOAM (right), is compared to results from COMSOL (left) and TUDelft (centre) models (Fiorina et al., 2014). A good agreement on the temperature field prediction can be appreciated, especially with the COMSOL results.

The mesh adopted for the spatial discretization in OpenFOAM is shown in Fig. 10. In Fig. 11, the details of computational mesh close to the core inlet zone are depicted. Details about the spatial discretization adopted in the COMSOL and TUDelft models can be found in Fiorina et al. (2014).

In Fig. 12, the evolution of the total reactor power after the step-wise reactivity insertion of 200 pcm is shown, as predicted by OpenFOAM, COMSOL and TUDelft models (Fiorina et al., 2014). The simulations refer to the simplified 2D, axial-symmetric MSFR test case,[3] and the *k*-epsilon turbulence model has been adopted in the three different tools. This turbulence model has been selected for the comparison because of its availability in both COMSOL and TUDelft tools.

A step-wise reactivity insertion represents a particularly demanding transient analysis from a numerical point of view, thus representing a good test for the models. Moreover, the insertion of 200 pcm leads to a super-prompt-critical condition, which involves a relevant power excursion and a considerable release of energy in a limited

[3] Details about simplified 2D, axial-symmetric MSFR geometry can be found in Brovchenko et al. (2013).

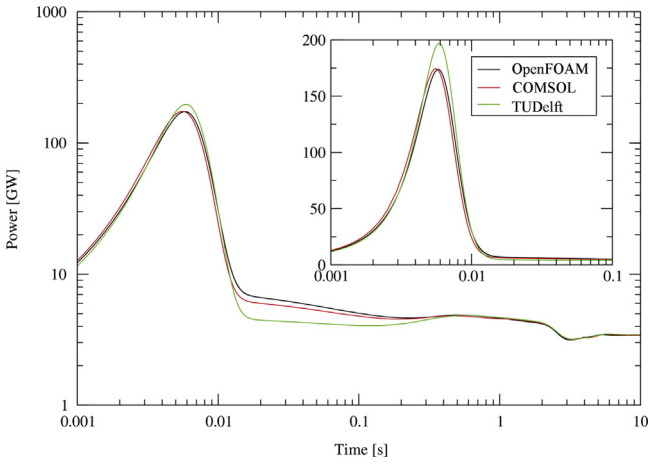

Fig. 12. Power excursion after step-wise insertion of 200 pcm of reactivity. Comparison among OpenFOAM, COMSOL and TUDelft models. Simplified 2D, axial-symmetric MSFR test case.

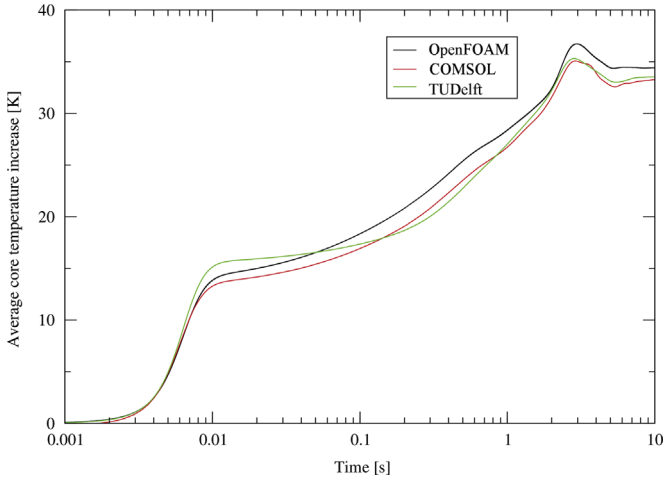

Fig. 13. Average core temperature after step-wise insertion of 200 pcm of reactivity. Comparison among OpenFOAM, COMSOL and TUDelft models. Simplified 2D, axial-symmetric MSFR test case.

time interval. In the OpenFOAM model, adaptive time stepping has been used thanks to the embedded error estimation provided by the fourth order implicit time integration scheme adopted.

In Fig. 13, the average core temperature for the analysed test case is shown as predicted by the three codes.

The prompt power rise triggered by the reactivity insertion leads to a rapid temperature increase. The consequent negative reactivity insertion due to Doppler and density feedbacks quickly reduces and stabilizes the power.

A good agreement between the three solutions can be appreciated in both power and average temperature predictions. In particular, the evolution of power for the OpenFOAM and COMSOL models agrees very well even in the prompt rise. The COMSOL model features the adoption of multi-group neutron diffusion. Moreover, the solution domain is extended also to the blanket and reflectors, and the compressible formulation of RANS equations is used. As pointed out in Section 3, the OpenFOAM model features several simplifications aimed at the reduction of the computational requirements, namely the reduction of the computational domain via the adoption of the albedo boundary conditions, the adoption of the one-speed neutron diffusion theory and the simplification of CFD solution by means of the Boussinesq approximation for the buoyancy effects. The fair agreement between COMSOL and OpenFOAM results can be considered as an *a posteriori* verification of the adopted approximations, regarding the considered conditions. TUDelft model predicts a slightly higher power excursion. This difference is in accordance with the lower effective delayed neutron fraction value obtained with this model as discussed in Fiorina et al. (2014).

4.2. Unprotected single pump failure

Different from previously published works (e.g., Fiorina et al., 2014), the present tool is able to deal with full core 3D MSFR geometries and can be useful to analyse asymmetric transient in which axial-symmetric simulations are not suitable. As an example of the capability of the model, a single pump failure accident is studied.

In the simulated accidental scenario, one of the 16 MSFR primary pumps undergoes a sudden bearing failure, which leads to its immediate blockage. Dealing with an unprotected scenario, no actions are taken in order to mitigate the consequences of the pump failure. In particular, the flow rate and the temperature of the intermediate salt in the heat exchanger of the broken branch are kept at nominal conditions. Results have been obtained adopting the full-core 3D geometry.

In Fig. 14, the evolution of relevant quantities in the analysed accidental scenario is shown. The green line shows the flow rate in the broken branch. After bearing failure, the head losses of the blocked pump and the heat exchanger lead to a rapid decrease of the flow rate. Buoyancy effects, along with hydrodynamic effects due to neighbouring branches, provide enough thrust to keep about 10% of the nominal flow in the broken pump. The total reactor power (black line) and the average core inlet and outlet temperatures (dashed blue and red lines) are slightly affected by the single pump failure. The MSFR operating conditions deviate little from nominal ones. Nonetheless, a potential unsafe behaviour can be appreciated analysing the temperatures relative to the broken branch. In particular, solid red and blue lines show the inlet and the outlet temperature of the heat exchanger located above the blocked pump, respectively. Due to mixing effects in the reactor core, the HEX inlet temperature remains close to the nominal value. On the other hand, due to the reduced flow rate

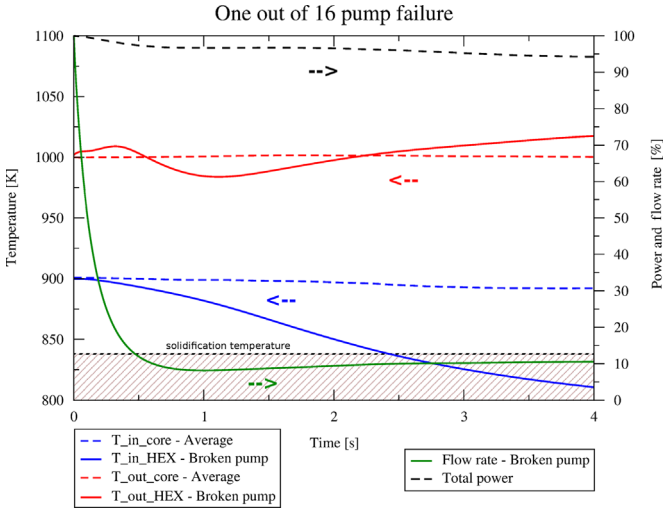

Fig. 14. Single pump failure unprotected scenario. Temperatures, flow rate and power. Solid lines refer to values relative to the broken pump loop. Dashed lines refer to reactor average values. (For interpretation of the references to colour in this figure caption, the reader is referred to the web version of this paper.)

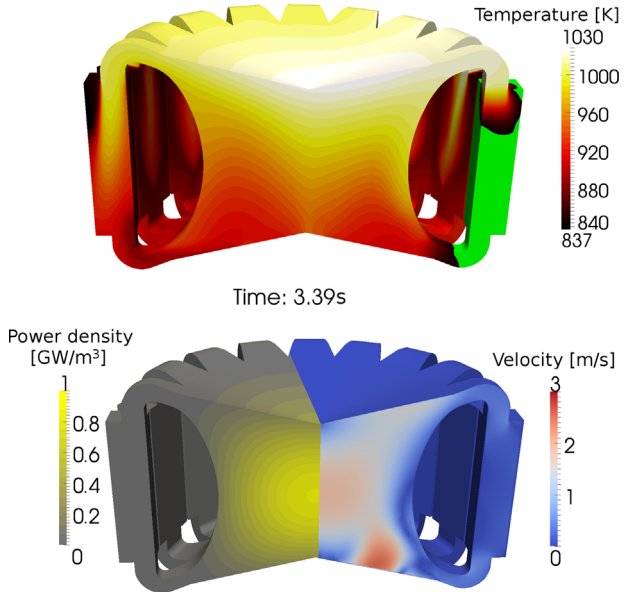

Fig. 15. Temperature (top), velocity and power density (bottom) fields in the MSFR after the single pump failure accident. (For interpretation of the references to colour in this figure caption, the reader is referred to the web version of this paper.)

in the broken branch and the nominal operation of the intermediate circuit, the temperature of the salt quickly reduces at the heat exchanger exit. If no action is taken promptly in a few seconds the HEX outlet temperature goes below the salt solidification temperature.

Fig. 15 shows the temperature (top), velocity and power density (bottom) fields in the MSFR about 3.4 s after the single pump failure accident. Temperature below melting point ($\sim$837 K) is highlighted in green. It can be appreciated that in a few seconds, most of the volume of the heat exchanger reaches almost stagnation conditions and solidification temperature. Despite the simplification adopted in the HEX modelling and the inability of the present tool to model salt phase change, the emergence of possible unsafe conditions as a consequence of a single pump failure is evident. Several mitigating features can be implemented in the MSFR design in order to limit or avoid solidification in different accidental scenarios (Geoffroy and Aufiero, 2013). Among these, the increase of the nominal intermediate salt temperature or the addition of HEX by-pass area seems promising.

5. Conclusion

In the analysis of the Molten Salt Fast Reactor behaviour, the presence of a strong coupling between neutronics and thermal-hydraulics and fast time scales calls for the adoption of coupling techniques which are more suitable than the common operator-splitting approach. Recent works also highlighted the significant impact of CFD modelling on the MSFR analysis and the need to adopt accurate turbulence models and realistic three-dimensional geometries.

In the present paper, the development of a multiphysics solver adopting the finite-volume open-source C++ library OpenFOAM is discussed. The work has been focused on the implementation of an accurate time-integration scheme and the adoption of suitable strategies and simplifications to enable a fast-running simulation of accidental transient on detailed full-core 3D geometries.

The neutronics capability of the multiphysics model have been assessed against Monte Carlo simulations, showing an adequate accuracy of the spatial neutron flux for the purpose of the analysis of accidental scenarios.

A super-prompt-critical reactivity insertion has been simulated with the proposed solver on a simplified geometry, for which results were already available in the literature, showing a good agreement with multiphysics models previously developed at Politecnico di Milano and Delft University of Technology.

An unprotected single pump failure accidental scenario has been simulated. Although the general reactor behaviour (total power and average temperatures) deviates only slightly from the nominal operating conditions, the results of the simulation show that unsafe situations might emerge as a consequence of the possible salt freezing in the broken circuit. This transient has been discussed an example of the capability of the model, while detailed safety analysis is beyond the scope of the present work and would require layout specifications of the core and fuel circuit components, which are not available in this pre-conceptual design of the MSFR.

In this view, the present multiphysics full-core modelling tool, which is able to describe the transient flow field and neutronics behaviour of the MSFR, might be of relevant interest in the phase of reactor design optimization, as shown by some preliminary analysis performed in the present work.

Accurate studies on turbulent mass transport and flow mixing in the MSFR operating conditions are not available at present, and would be required to assess the suitability of the adopted RANS turbulence models.

In addition to computationally lightweight and versatile solvers, aimed at the simulation of transient incidental scenarios, more accurate models are envisaged to provide reference solutions. For this reason, a research activity is ongoing among some of the authors and other groups to develop multiphysics tools for fast-spectrum circulating-fuels reactors, taking advantage of more refined neutron transport modelling, via both deterministic and Monte Carlo approaches.

Acknowledgements

The authors would like to thank Axel Laureau, Pablo Rubiolo (LPSC - France) and Ivor Clifford (PSI - Switzerland) for fruitful discussion and criticism.

This work was financially supported by Politecnico di Milano via the PhD Grant of Manuele Aufiero entitled “International Mobility 2012/2013”, in the frame of the Doctoral Program in “Energy and Nuclear Science and Technology 26 cycle”.

This work has also been supported by CINECA supercomputing center under ISCRA Project MPMCF - *Multi-Physics Modelling of Circulating-Fuel Nuclear Reactors*, by Regione Lombardia and CILEA supercomputing center under LISA Project CFMC - *Simulazioni Monte Carlo per reattori a sali fusi*, and by an Amazon Web Services (AWS) in Education grant award.

Appendix

In the following, a brief summary of the main equations that are discretized and solved in the OpenFOAM multiphysics model is given.

The neutronics model of the MSFR involves the solution of the one-group neutron diffusion:

$$\frac{1}{v}\frac{\partial \phi}{\partial t} = \nabla \cdot D\nabla\phi - \Sigma_a\phi + (1-\beta_{tot})\nu\Sigma_f\phi + \sum_{i=1}^{8}\lambda_i c_i \quad (1)$$

where ϕ is the neutron flux, β_{tot} is the total delayed neutron fraction, v is the average neutron velocity, D is the diffusion

coefficient, and Σ_a and $\nu\Sigma_f$ are the absorption and the neutron production cross-sections, respectively. c_i is the delayed neutron precursor concentration of the ith group, and λ_i and β_i are the relative decay constant and delayed neutron fraction, respectively.

As simple example of the equation implementation, Eq. (1) is discretized and solved in OpenFOAM adopting the following lines of code:

```
solve
(
      fvm::ddt(IV,phi)
      ==
      fvm::laplacian(D,phi)
    + fvm::Sp((nu_prompt * Sigma_F),phi)
    - fvm::Sp(Sigma_A,phi)
    + delayedNeutronSource
);
```

The different terms of this top-level C++ implementations closely parallel their mathematical counterparts. The term `fvm::ddt(IV,phi)` is the equivalent of $(1/v)\partial\phi/\partial t$, where `IV` represents the inverse neutron velocity $(1/v)$ and `phi` is the one-group scalar neutron flux (ϕ). The fission neutron production operator $((1-\beta_{tot})\nu\Sigma_f)$ and the neutron absorption operator (Σ_a) have been introduced as implicit terms in the solution matrix by means of the lines: `fvm::Sp((nu_prompt * Sigma_F),phi)` and `fvm::Sp(Sigma_A,phi)`. Neutron diffusion is modelled by means of the Laplacian operator `fvm::laplacian(D,phi)`. Thanks to the flexibility of the OpenFOAM (2013) library, several standard spatial discretization schemes can be selected and adopted in the solver at runtime.

The dependencies of the cross-sections on the fuel temperature T and density ρ have been introduced as follows:

$$\Sigma(T,\rho)=\left(\frac{\rho}{\rho_0}\right)\left[\Sigma_0+\alpha_\Sigma\log\left(\frac{T}{T_0}\right)\right] \tag{2}$$

$$D(T,\rho)=\left(\frac{\rho_0}{\rho}\right)\left[D_0+\alpha_D\log\left(\frac{T}{T_0}\right)\right] \tag{3}$$

where T_0 is the fuel reference temperature and ρ_0 is the fuel density at the reference temperature. In order to limit the computational domain to the fuel circuit only, albedo boundary conditions have been adopted both in the upper and lower limits of the core:

$$\mathbf{n}\cdot(D\nabla\phi)_b=-\gamma\phi_b \tag{4}$$

All the group constants and their temperature dependencies (α_D and α_Σ), as well as the albedo coefficients (γ), have been calculated by means of SERPENT. Delayed neutrons have been considered through the precursor balance equations for the 8 delayed neutron groups of the JEFF-3.1 library (Koning et al., 2006):

$$\frac{\partial c_i}{\partial t}=-\nabla(\mathbf{u}c_i)+\nabla\cdot\frac{\nu_T}{Sc_T}\nabla c_i-\lambda_i c_i+\beta_i\cdot\nu\Sigma_f\phi \tag{5}$$

In a similar way, the balance equations for the decay heat precursors have been introduced in the model:

$$\frac{\partial d_i}{\partial t}=-\nabla(\mathbf{u}d_i)+\nabla\cdot\frac{\nu_T}{Sc_T}\nabla d_i-\lambda_{heat,i}\cdot d_i+\beta_{heat,i}E_f\Sigma_f\phi \tag{6}$$

In Eqs. (5) and (6), d_i, $\lambda_{heat,i}$ and $\beta_{heat,i}$ are the concentration, decay constant and fraction of the ith decay heat precursor. E_f represents the average energy released per fission, and $\mathbf{u}$ is the fuel salt velocity. Sc_T is the turbulent Schmidt number, which has been assumed to be equal to 0.85 in the present work.

The temperature field in the MSFR fuel circuit has been solved introducing the energy balance equation as follows:

$$\frac{\partial T}{\partial t}=-\nabla(\mathbf{u}T)+\nabla\cdot\frac{(K_{salt}+K_T)}{\rho C_p}\nabla T+(1-\beta_{heat,tot})\frac{E_f}{\rho C_p}\Sigma_f\phi+\sum_{i=1}^{3}\frac{\lambda_{heat,i}}{\rho C_p}d_i \tag{7}$$

The terms K_{salt} and K_T refer to the laminar and the turbulent salt thermal conductivity, respectively. The latter is calculated with a constant and a uniform turbulent Prandtl number equal to 0.85. ρ and C_p are the fluid density and the specific heat, respectively.

Homogeneous Neumann boundary conditions have been adopted at the walls of the fuel circuit for temperature and concentration of delayed neutrons and decay heat precursors.

The model of the fluid flow is based on the incompressible form of the Reynolds-Averaged Navier–Stokes (RANS) equations. The proposed tool fully benefits from the availability of pre-implemented turbulence models and wall functions in OpenFOAM. In particular, the comparisons shown in Section 4.1 have been obtained adopting the standard k-epsilon model, which is also available in COMSOL and TUDelft simulation tools, whereas the other results of the present work have been achieved by means of the *realizable* k-epsilon model, which is thought to be more accurate for the MSFR flow conditions.

References

Aufiero, M., 2014. Development of Advanced Simulation Tools for Circulating-Fuel Nuclear Reactors (Ph.D. thesis). Politecnico di Milano.

Aufiero, M., Brovchenko, M., Cammi, A., Clifford, I., Geoffroy, O., Heuer, D., Laureau, A., Losa, M., Luzzi, L., Merle-Lucotte, E., Ricotti, M.E., Rouch, H., 2014. Calculating the effective delayed neutron fraction in the molten salt fast reactor: analytical, deterministic and monte carlo approaches. Ann. Nucl. Energy 65, 78–90.

Aufiero, M., Cammi, A., Fiorina, C., Leppänen, J., Luzzi, L., Ricotti, M., 2013. An extended version of the SERPENT-2 code to investigate fuel burn-up and core material evolution of the Molten Salt Fast Reactor. J. Nucl. Mater. 441 (1–3), 473–486.

Avramova, M.N., Ivanov, K.N., 1997. Verification, validation and uncertainty quantification in multi-physics modeling for nuclear reactor design and safety analysis. Int. J. Heat Mass Transf. 40, 4191–4196.

Brovchenko, M., Heuer, D., Merle-Lucotte, E., Allibert, M., Capellan, N., Ghetta, V., Laureau, A., 2012. Preliminary safety calculations to improve the design of Molten Salt Fast Reactor. In: Proceedings of PHYSOR 2012, Knoxville, TN, USA, April 15–20, 2012.

Brovchenko, M., Merle-Lucotte, E., Rouch, H., Alcaro, F., Aufiero, M., Cammi, A., Dulla, S., Feynberg, O., Frima, L., Geoffroy, O., Heuer, D., Ignatiev, V., Kloosterman, J.-L., Lathouwers, D., Laureau, A., Luzzi, L., Merk, B., Ravetto, P., Rineiski, A., Rubiolo, P., Rui, L., Szieberth, M., Wang, S., Yamaji, B., et al., 2013. Optimization of the Pre-Conceptual Design of the MSFR—EVOL Project. Deliverable D2.2.

Cammi, A., DiMarcello, V., Luzzi, L., Memoli, V., Ricotti, M.E., 2011. A multi-physics modelling approach to the dynamics of molten salt reactors. Ann. Nucl. Energy 38, 1356–1372.

Clifford, I., Jasak, H., 2009. The application of a multi-physics toolkit to spatial reactor dynamics. In: 2009 International Conference on Mathematics, Computational Methods & Reactor Physics (M&C 2009), Saratoga Springs, NY, USA, May 3–7, 2009.

Duderstadt, J.J., Hamilton, L.J., 1976. Nuclear Reactor Analysis. John Wiley and Sons, New York

EVOL, 2010–2013. Evaluation and Viability of Liquid fuel fast reactor system. Available at: ⟨http://www.evol-project.org/⟩.

Fiorina, C., Aufiero, M., Cammi, A., Franceschini, F., Krepel, J., Luzzi, L., Mikityuk, K., Ricotti, M.E., 2013. Investigation of the MSFR core physics and fuel cycle characteristics. Prog. Nucl. Energy 68, 153–168.

Fiorina, C., Lathouwers, D., Aufiero, M., Cammi, A., Guerrieri, C., Kloosterman, J.L., Luzzi, L., Ricotti, M.E., 2014. Modelling and analysis of the MSFR transient behaviour. Ann. Nucl. Energy 64, 485–498.

Geoffroy, O., Aufiero, M., 2013. A few comments on the MSFR safety and design optimization. In: Presented at the EVOL WP2 Workshop+EVOL Meeting, Grenoble, France. Available at: ⟨http://indico.in2p3.fr/conferenceOtherViews.py?confId=8432⟩.

GIF, 2010. Generation IV International Forum, Annual Report. Available at: ⟨http://www.gen-4.org/PDFs/GIF-2010-Annual-Report.pdf⟩.

Jasak, H., Jemcov, A., Tukovic, Z., 2007. OpenFOAM: a C++ library for complex physics simulations. In: International Workshop on Coupled Methods in Numerical Dynamics. IUC, Dubrovnik, Croatia, September 19–21, 2007.

Kennedy, C.A., Carpenter, M.H., 2003. Additive Runge–Kutta schemes for convection–diffusion–reaction equations. Appl. Numer. Math. 44 (1–2), 139–181.

Koning, A., Forrest, R., Kellett, M., Mills, R., Henriksson, H., Rugama, Y., 2006. The JEFF-3.1 Nuclear Data Library. Technical Report, JEFF Report 21, NEA—OECD.
Losa, M., 2013. Multiphisics Modelling of the Molten Salt Fast Reactor: Comparison of Three Turbulence Models (Master's thesis). Universidad Politécnica de Madrid/Politecnico di Milano.
Mahadevan, V.S., Ragusa, J.C., Mousseau, V.A., 2012. A verification exercise in multiphysics simulations for coupled reactor physics calculations. Prog. Nucl. Energy 55, 12–32.
Merle-Lucotte, E., Heuer, D., Allibert, M., Brovchenko, M., Capellan, N., Ghetta, V., 2011. Launching the thorium fuel cycle with the molten salt fast reactor. In: Proceedings of ICAPP 2011, Nice, France, May 2–6, 2011.
Merle-Lucotte, E., Heuer, D., Allibert, M., Doligez, X., Ghetta, V., 2009. Optimizing the burning efficiency and the deployment capacities of the molten salt fast reactor. In: Proceedings of GLOBAL 2009, Paris, France, September 6–11, 2009.
OpenFOAM, 2013. OpenFOAM Documentation. Available at: ⟨http://www.openfoam.org/docs/⟩.
Ragusa, J.C., Mahadevan, V.S., 2009. Consistent and accurate schemes for coupled neutronics thermal-hydraulics reactor analysis. Nucl. Eng. Des. 239 (3), 566–579.
Rouch, H., Geoffroy, O., Rubiolo, P., Laureau, A., Brovchenko, M., Heuer, D., Merle-Lucotte, E., 2014. Preliminary thermal-hydraulic core design of the Molten Salt Fast Reactor MSFR. Ann. Nucl. Energy 64, 449–456.
Serp, J., Allibert, M., Beneš, O., Delpech, S., Feynberg, O., Ghetta, V., Heuer, D., Holcomb, D., Ignatiev,V., Kloosterman, J.L., Luzzi, L., Merle-Lucotte, E., Uhlíř, J., Yoshioka, R., Zhimin,D. The molten salt reactor (MSR) in generation IV: Overview and perspectives, Prog. Nucl. Energy (In Press), http://dx.doi.org/10.1016/j.pnucene.2014.02.014.
SERPENT, 2011. PSG2/Serpent Monte Carlo Reactor Physics Burnup Calculation Code. URL ⟨http://montecarlo.vtt.fi⟩.
Versteeg, H.K., Malalasekera, W., 2007. An Introduction to Computational Fluid Dynamics: The Finite Volume Method, Pearson Education Limited, Essex, England
Weller, H.G., Tabor, G., Jasak, H., Fureby, C., 1998. A tensorial approach to computational continuum mechanics using object-oriented techniques. Comput. Phys. 12, 620–631.